Published in final edited form as:
Curr Biol. 2012 March 6; 22(5): 353–362. doi:10.1016/j.cub.2012.01.007.

Loom sensitive neurons link computation to action in the *Drosophila* visual system

Saskia E. J. de Vries and **Thomas R. Clandinin***
Department of Neurobiology, Stanford University, Stanford, CA 94305

Summary

Background—Many animals extract specific cues from rich visual scenes to guide appropriate behaviors. Such cues include visual motion signals produced both by self movement and by moving objects in the environment. The complexity of these signals requires neural circuits to link particular patterns of motion to specific behavioral responses.

Results—Through electrophysiological recordings, we characterize genetically identified neurons in the optic lobe of *Drosophila* that are specifically tuned to detect motion signals produced by looming objects on a collision course with the fly. Using a genetic manipulation to specifically silence these neurons, we demonstrate that signals from these cells are important for flies to efficiently initiate the loom escape response. Moreover, through targeted expression of Channelrhodopsin in these cells, in flies that are blind, we reveal that optogenetic stimulation of these neurons is typically sufficient to elicit escape, even in the absence of any visual stimulus.

Conclusions—In this compact nervous system, a small group of neurons that extract a specific visual cue from local motion inputs serve to trigger the ethologically appropriate behavioral response.

Introduction

The brain must extract ethologically relevant cues from the sensory environment, and use this information to generate appropriate behavioral responses. How this sequence of neural transformations is achieved has been investigated in many contexts, focusing on sensory encoding of the stimulus, psychophysical analysis, and computational studies that link perception to behavior. Using a combination of single cell physiology, computational modeling and behavioral analysis, we describe a link between neurons that capture a specific sensory computation and the appropriate behavioral response using loom detection in the fruit fly as a model.

Animals use visual motion cues to maintain an appropriate movement trajectory and to avoid collisions or capture [1, 2]. In flies, the lobula complex, the third neuropil of the optic lobe, is thought to underlie such motion processing [3]. This complex comprises two ganglia, the lobula and the lobula plate, and contains a diverse array of cell types [4, 5]. While the visual response properties of many of these cells remain unknown [6], in *Drosophila* and other flies, electrophysiological studies of specific subsets of lobular

*Author for Correspondence: Fairchild D200, 299 W. Campus Drive, Stanford University, Stanford, CA 94305, Phone: (650) 723-7556, Fax: (650) 725-3958, trc@stanford.edu.

neurons, including lobula plate tangential cells (LPTCs) and small target motion detector neurons, have described cells that become tuned to specific patterns of movement through the integration of local motion cues [3, 7, 8]. Based on these tuning properties, these cells have been proposed to guide specific navigational behaviors relevant to these patterns. Consistent with this notion, ablation and microstimulation studies that have disrupted the activity of groups of these cells have demonstrated that they play roles in motion perception [9–12]. However, in no case has the activities of identified neurons in the lobula complex that are tuned to a particular pattern of motion been demonstrated to be critical to trigger the specific behavioral response appropriate to that signal.

Here we examine both the visual responses and behavioral role of a group of genetically identified neurons in the *Drosophila* lobula complex. These cells are tuned to detect looming stimuli, visual motion signals generated by an object on a direct collision course with the fly. The response properties of these cells display many similarities to loom detectors in other animals. Using reverse correlation and a Linear-Nonlinear modeling approach [13, 14], we describe the visual sensitivities of these cells. Looming stimuli elicit escape behaviors from flies [15–18], and other animals [1], allowing them to avoid imminent collisions. Using genetic tools to both silence and activate these specific neurons, we demonstrate a causal link between these loom detector neurons and the escape response of the fly. Thus, these neurons serve as the nexus that integrates specific motion cues and triggers the escape response in this sensorimotor pathway.

Results

Morphological characterization of Foma-1 neurons

Using a forward genetic screen, we identified a GAL-4 enhancer trap expressed in a small cluster of neurons innervating the lobula complex, the Foma-1 neurons, as well as the γ lobe of the mushroom body [19] (Figure 1A, 1B and 1C). This enhancer trap was typically expressed in five cells in each optic lobe, and iontophoretic injections of fluorescent dye into these cells revealed three distinct morphological types (Figure 1D–1K): a wide-field translobula-plate neuron [4], with processes in both the lobula and lobula plate (Figure 1D and 1H, n = 6); a wide-field lobula projection neuron [4, 5], with processes in a proximal layer of the lobula and a projection into the protocerebrum (Figure 1E and 1I, n = 4); and a cluster of three lobula plate tangential cells, with sparse processes in the lobula plate and an axonal projection into the central brain (Figure 1F and 1J, n = 6).

Mapping the receptive field of Foma-1 neurons

We targeted Foma-1 neurons for loose patch recordings [20] to examine their visual responses. We accessed the neurons from the posterior of the fly's head, while presenting visual stimuli generated on a high-speed CRT monitor to the eyes via two coherent fiber optic bundles (Figure S2). Due to the stereotyped locations of the neuronal cell bodies, we could reproducibly target individual cells expressing GFP under the control of Foma-1GAL-4. Of the five cells, we were able to record from the three largest cell bodies, verified by dye injection into the cell body following every recording, and obtained reproducible spiking responses to visual stimuli presented within the spatial extent of our display (n = 79). While these cells are morphologically distinct, their responses, as we will describe, were indistinguishable. We confirmed the identities of two recorded cells through dye labeling of the processes following data collection for the translobula-plate cell and the lobula projection neuron (data not shown).

We presented a variety of visual stimuli to the fly, examining the luminance and motion sensitivity of these cells (Figure 2). They responded to both increases and decreases in

global light intensity (Figure 2A and 2D), and were sensitive to the onset and offset of local flashes of light within a dorsal region of the visual field (Figure 2B and 2E). Within this receptive field, these cells also responded in a direction selective fashion to the movement of a small dot, preferring downward motion (Figure 2C, 2F and Figure S1). However, these neurons did not exhibit direction selective responses to global motion stimuli, neither to drifting gratings nor to a dynamic dot stimulus (Figure S1).

Foma-1 neurons detect looming stimuli

Foma-1 neurons did, however, exhibit strong, selective responses to looming stimuli that mimicked an object on a direct collision course. Such stimuli expand as a function of the object's size and speed (Figure 3A and 3B). When the fly was presented with such a stimulus, the Foma-1 neurons' firing rate increased until it reached a peak close to the anticipated time of collision, whereupon there was a marked suppression of spiking activity (Figure 3C). This shape of this response was the same regardless of whether the looming object persisted or disappeared upon reaching its final angle (Figure S2). This response is broadly similar to those of loom detectors found in locust [21–23], pigeon [24, 25], and other animals [26–29]. Further, this response was similar to loom sensitive activity recorded in the ventral nerve cord of *Drosophila*, whose peak firing rate was correlated with the timing of the flies' escape response [17].

Many loom detectors exhibit four characteristic features. First, the time of the peak firing rate relative to the expected time of collision is linearly related to the ratio of the object's size to its velocity towards the animal, $l/|v|$. As previous studies have described, this linear relationship suggests that these neurons implement an arithmetic multiplication, and act as angular threshold detectors such that the peak response occurs at a fixed delay after the stimulus reaches a given angle [30, 31]. Second, loom detectors respond with the same timing to looming stimuli that originate in different locations of the visual field. Third, for a loom detector, the time of peak firing rate is not affected by the contrast polarity of the object. Finally, a loom detector responds to an approaching object even when its approach does not cause a global change in luminance.

Foma-1 neurons exhibited all four of these characteristics. First, the time of the peak firing rate was linearly related to the ratio of the object's size to its velocity towards the fly, $l/|v|$ (Figure 3D). Second, these neurons responded identically to looming stimuli that originated in different locations within the visual field (Figure 3E, 3F, and S2). We compared looming stimuli that initiated near the dorsal edge of the visual field with those that began frontally. In these experiments, the edge of the looming dot that began at the dorsal periphery passed through the receptive field in the preferred direction of local motion, while the edge of the looming dot that began frontally passed through the receptive field in the non-preferred direction. If the local motion preferences (Figure S1) were sufficient to account for the loom response, this difference in initial position would elicit opposite responses. However, this was not the case: Foma-1 neurons responded almost identically to these two stimuli, both in their overall firing rate and in the timing of the peak response (Figure 3E and 3F). Moreover, varying the azimuthal position of the frontal stimuli, which would also change the pattern of expansion relative to the local motion preferences, also did not change the response (Figure S2). Third, these neurons responded to looming stimuli that were either brighter than the background (contrast increment) or dimmer than the background (contrast decrement) (Figure 3G). While the firing rate evoked by these two stimuli differed, the timing of the peak response was unchanged (Figure 3H). Finally, these cells responded strongly to the looming approach of a "checkerboard" stimulus comprising squares of alternating light and dark contrast against a gray background (Figure 3I and 3J). As the response of cells to this equiluminant stimulus was the same as that to a looming white object on a gray background (a stimulus that brightens as the object approaches) we infer that Foma-1 neurons can

respond to looming cues in the absence of global luminance changes. Based on these criteria, the Foma-1 enhancer trap labels a small group of loom detecting neurons, thus providing a genetic entry point to the dissection of the circuit that underlies this computation.

The angular threshold for a loom detector can be computed from the parameters of the linear fit between peak firing rate and $l/|v|$ [31]. Using this analysis, our data predict an angular threshold of 67.6 ± 2.5° (mean ± s.e.m., see Methods), an unusually large threshold, greater than those of loom sensitive activity in *Drosophila* and other species [17, 28, 31]. To directly test this angular threshold we presented looming stimuli that ceased to expand before reaching this size, and found that cells did indeed respond to this truncated looming stimulus (n = 3 out of 5 cells responded, Figure S2). Thus, this parameter appears to provide an incomplete description of the response threshold of these particular cells.

Developing a quantitative model of Foma-1 looming responses

To more completely characterize the response to approaching stimuli, we created a random looming stimulus in which a virtual object jittered towards and away from the fly, its velocity being chosen from a uniform distribution every 25ms. This stimulus samples a wide range of approach trajectory statistics, and hence should provide an extensive exploration of a loom detector's tuning properties. We used spike triggered analysis to compute a Linear-Nonlinear (LN) model of the stimulus-response function [13] (Figure 4A; see Methods). This model uses two functions to predict a cell's response to the stimulus: a linear filter and a static nonlinearity. The linear filter captures the neuron's sensitivity to the visual angle of the stimulus as a function of time, while the static nonlinearity captures nonlinearities in the neuron's response, including its gain and threshold. The Foma-1 neurons responded robustly to the random looming stimulus, and the LN model captured this response well such that the LN prediction matched the firing rate as well as the trial-to-trial noise in the response (Figure 4B, See Methods). This model also accurately predicted the timing and magnitude of the cells' responses to presentations of a looming stimulus comprising an isolated dot on a direct approach trajectory (as used in Figure 3; data not shown, Pearson's correlation coefficient 0.53 ± 0.02 (mean ± s.e.m.), n = 14).

To test the ability of this model to capture the characteristic features of a loom detector, we calculated the LN model using a random looming stimulus that originated either at the dorsal periphery or anteriorally in the visual field. Both the linear filters (Figure 4C) and the static nonlinearities (Figure 4D) were indistinguishable between these two conditions, further confirming the position invariance of the neurons' responses. We also calculated the LN model under both contrast increment and decrement conditions. For both conditions we observed a linear filter with positive polarity (Figure 4E), indicating that the Foma-1 neurons responded to increasing angle of the dot regardless of its contrast.

However, the filter calculated under the contrast decrement condition was slower than that for contrast increment, with a peak sensitivity 20 ± 4 ms after that for contrast increment (mean ± s.e.m., n = 6). Such temporal differences could result from luminance sensitivity differences in motion detecting pathways [32, 33]. The static nonlinearity for the contrast decrement condition reveals a lower gain than for the contrast increment (Figure 4F). This is consistent with the lower firing rate observed when a dark dot approaches with constant velocity (Figure 3G). Finally, the linear filter (Figure 4G) and nonlinearities (Figure 4H) we calculated using a white dot or an equiluminant checkerboard stimulus were very similar. Thus, the LN loom model captures the response selectivity of Foma-1 neurons and can robustly predict their responses to looming stimuli of varied velocities and trajectories.

While our experiments using looming checkerboard stimuli demonstrate that Foma-1 cells can respond to looming in the absence of global luminance change they are insufficient to exclude the possibility that luminance changes might nonetheless contribute to the loom response. To quantitatively examine this possibility, we computed a LN model to a full field flicker stimulus (Figure 5A). The luminance of the monitor was chosen at random from a Gaussian distribution every 15ms, and thus constitutes a pure luminance stimulus with no looming component. The resulting model, therefore, captures the neuron's sensitivity to luminance (Figure 5A). We then used this luminance model to predict the neurons' responses to the random looming stimuli, for both bright and dark dots. We calculated the luminance changes in the random looming stimuli, and used this as the input for the luminance LN model (Figure 5B – 5G). We found that the LN_{loom} model (see Figure 4) more accurately predicted the response of the Foma-1 neurons to the random loom stimuli than the $LN_{luminance}$ model. In particular, the LN_{loom} model better captured the predicted firing rate of Foma-1 neurons to the contrast increment stimulus, and better captured both the timing and the firing rate of the neurons' activity to contrast decrements (Figure 5C, 5D, 5F, 5G). Thus the responses of Foma-1 neurons are mainly induced by increasing angle and not by luminance changes.

Defining the behavioral role of Foma-1 neurons

As our LN_{loom} model contains a simple thresholded nonlinearity, we suggest that increasing the firing rate of the loom detecting neurons above this threshold serves to increase the probability of evoking a behavioral response. To test the functional requirements of Foma-1 neurons for behavior, we took advantage of the fact that *Drosophila* exhibit a robust escape response to looming stimuli, an ethologically relevant cue under many circumstances, including predator evasion. When presented with a looming stimulus, flies take off into flight [15–18]. Based on these previous behavioral studies, we constructed an apparatus that presented a computer-generated looming stimulus to individual flies (Figure 6A and Figure S3). High speed imaging revealed details specific to escape behavior, including raised wings prior to takeoff and a subsequent unstable flight trajectory [15, 16, 18] (Figure 6B, Movie S1). Specifically, 92% (n = 50 filmed takeoffs) of flies exhibited raised wings prior to takeoff. Under these conditions, a loom escape response was elicited from approximately 65–76% of control flies, depending on genotype (Figure 6C). In addition these escapes displayed a linear $l/|v|$ relationship (Figure S3).

To directly demonstrate that these responses corresponded to visually-evoked escapes, we first silenced L2 neurons by expressing *shibire*^{ts}, a temperature sensitive synaptic silencer [34], in these cells. L2 neurons are lamina monopolar cells that are immediate post-synaptic targets of photoreceptors, and are critical for detecting the movement of dark edges [19, 32, 33, 35]. Under these conditions, escape behavior was strongly suppressed such that only 11% of flies jumped when presented with the looming stimulus (Figure 6C). Next, we tested whether the activity of Foma-1 neurons influenced this escape behavior by silencing these cells in the same manner. Under these conditions, only 30% of the flies jumped in response to the looming stimulus, a significant decrease relative to control flies (Figure 6C). By comparison with control flies, which typically escaped within the first or second presentation of the loom stimulus, flies with silenced Foma-1 neurons that did takeoff were as likely to escape to any of the six stimulus presentations (Figure S3). Thus, Foma-1 neurons are important for the normal frequency of initiation of the wild-type loom escape behavior.

If increasing the activity of Foma-1 neurons signified the presence of a looming stimulus, targeted stimulation of these cells should induce escape behavior in the absence of visual input. We therefore expressed channelrhodopsin in Foma-1 neurons and used light to selectively activate these cells [36]. To eliminate any photoreceptor mediated visual

responses, we rendered flies blind using a null allele of a critical component of the phototransduction cascade, Phospholipase C-β, encoded by the *norpA* gene [37]. We then illuminated individual flies with blue light to evoke escape responses (Figure 6D and Figure S3). Under these conditions, blue light illumination induced escape responses that were behaviorally similar to those we observed with looming stimuli, with 90% of flies (n = 30) raising their wings prior to takeoff (Figure 6E, Movie S2). Quantitatively, while only 16–21% of control blind flies, depending on genotype, took off within a five second interval, 75% of flies that expressed channelrhodopsin in Foma-1 neurons did so (Figure 6F). Thus, stimulation of Foma-1 neurons was typically sufficient to evoke escape behavior, even when no visual input was present. To test whether such a strong behavioral response was specific to the activation of the Foma-1 neurons, we took advantage of cell-specific Gal4 elements that could target expression of channelrhodopsin to other neuron types (thereby providing specific access to the activation of these cells). Importantly, channelrhodopsin mediated stimulation of the -lobe of the mushroom body, the only other brain region in which Foma-1GAL-4 is expressed, did not significantly increase the frequency of escape response (Figure 6F). Finally, selective activation of L2 neurons was also insufficient to evoke escape responses (Figure 6F). Thus, while these cells are necessary for loom escape behavior, their outputs are not sufficiently specialized to evoke this particular response. These data argue strongly that escapes evoked by stimulation of Foma-1 neurons require the integration of motion signals that are specific to loom, information that is unavailable earlier in the visual pathway.

Discussion

Collision detection and avoidance has provided a powerful model for studying sensorimotor integration, as the behavior is ethologically constrained, and loom sensitive neurons have been found in many animals [1]. While previous studies have demonstrated that fruit flies exhibit escape responses to looming stimuli and display loom sensitive activities [15–18], our studies have identified a small group of neurons that perform this computation, thereby providing a genetic entrypoint for dissecting this sensorimotor pathway. Moreover, we demonstrate that the outputs of these cells are important to trigger the appropriate escape response, establishing a sensorimotor link for collision detection and avoidance.

Neurons sensitive to looming stimuli can be tuned to different optical variables of the stimulus. Some loom-sensitive neurons, found in the pigeon tectum, respond to the relative rate of expansion, responses that are marked by a fixed time of response onset preceding collision, regardless of the size or speed of the approaching object [24, 25]. Other neurons exhibit a scaling response, in which one optical variable is scaled by the exponential of the visual angle of the object. These responses, observed in the lobula giant movement detectors (LGMD) neurons in locusts, Mauthner cells in goldfish, as well as in loom sensitive neurons in other species [17, 21, 24, 27–29], depend on the relative speed of the approaching object, such that they exhibit a linear relationship between the time of peak response and $l/|v|$. The Foma-1 neurons exhibit responses consistent with this latter category.

Perhaps the best studied of such scaling loom-detectors are the LGMD neurons, large cells situated in the lobula of the locust. These cells respond to translational motion, and to the motion of small objects, but are not directionally selective for global motion [38–40]. These neurons have large receptive fields that cover most of the ipsilateral visual field, and are most sensitive along the visual equator and in the caudal region of the visual field [41]. They respond robustly to looming stimuli, and are both contrast and position invariant [22]. The LGMD neurons, and the descending contralateral movement detector (DCMD) they synapse onto, are strongly correlated with the escape behavior of locusts, their peak activity tightly matching the time of the locusts takeoff in response to a looming stimulus [26].

Foma-1 neurons exhibit many similarities to LGMD neurons, showing similar responses to motion and looming stimuli. However, there are also significant differences. In particular, the receptive field of Foma-1 neurons is strongest in the dorsal region of the visual field, while that of LGMD neurons is along the visual equator. In addition, unlike LGMD, the time of peak firing rate for the Foma-1 neurons occurs after the expected time of collision for most of the $l/|v|$ conditions tested, and invariably after the time of takeoff. Taken together with the fact that silencing Foma-1 neurons did not completely eliminate the loom escape behavior, these results are consistent with the notion that there are multiple pathways for loom detection in fruit flies, perhaps reflecting the ethological importance of this behavioral response.

Foma-1 neurons were originally identified using a behavioral assay that measured responses to global motion stimuli [19]. Based on that assay, the Foma-1 neurons were found to affect the turning responses of the flies. In that context, the global dynamic dot motion stimulus has both an acceleration component and an expansion component. Based on our measurements, the expansion component in these particular stimuli were likely insufficient to elicit the looming response of these neurons. However, edge acceleration has been shown to play a key role in driving the responses of LGMD neurons [42, 43]. We therefore believe that the imbalances in the acceleration and/or expansion components of the global motion stimulus between the two eyes could cause the rotational phenotypes associated with silencing Foma-1 neurons as previously reported [19]. Consistent with this, looming signals trigger saccadic turns in flying flies when presented unilaterally [44, 45].

Detection of a looming object requires using motion signals to extract information about relative speed and trajectory. Recent efforts have begun to shed light on the structure of such local motion detecting circuits in the fruit fly using tools that are uniquely available in this genetic model [46]. In the context of optomotor responses, these elementary detectors are thought to converge on LPTCs to shape course control via feedback provided by global patterns of motion associated with self-movement, such that each LPTCs global motion response results from the spatial summation of local motion inputs [3]. Our data suggest that these peripheral local motion detecting pathways also converge on the Foma-1 neurons to direct escape responses to looming objects. However, as the local motion preferences of Foma-1 neurons cannot account for their loom responses, these local motion inputs must be integrated in a novel way by Foma-1 neurons. As the Linear-Nonlinear model we describe accurately captures the response properties of these loom detectors, predicting the neurons' responses to collisions at varying velocities, it provides a computational framework for assessing how these converging neural circuits shape these responses. Future genetic manipulations of these circuits, combined with this model, will reveal how local motion cues are integrated into the looming signal, defining the mechanisms of information processing in this sensorimotor pathway.

The richness of visual scenes, combined with the breadth of an animal's behavioral repertoire, demands a neural mechanism linking specific visual features to particular behavioral responses. Visual motion patterns are themselves complex, having translational, rotational and expansion components resulting from both self movement and moving objects. The ethologically appropriate behavioral response to such cues is highly dependent on the precise structure of the motion pattern. As the lobula complex is one of the earliest stages in visual processing at which the outputs of motion detectors distributed across visual space can be collectively analyzed, cells in this area present perhaps the first opportunity for the fly brain to directly link specific combinations of motion cues to appropriate behavioral responses. Remarkably, activation of just a small number of cells in this area is sufficient to elicit the precise sequence of coordinated, complex motor outputs that define the escape response. More broadly, our studies provide causal evidence that the relatively small number

of output pathways from this area into the central brain encode information that has direct, specific access to the animal's behavioral repertoire. That is, we anticipate that the tuning properties of other neurons in these areas will be similarly aligned with their roles in triggering different, specific behaviors.

Behaviorally relevant visual information, motion included, can typically only be deduced by analyzing patterns of photoreceptor activation over space and time. The sophistication of this analysis is undoubtedly reflected in the size and complexity of the visual circuitry immediately downstream of photoreceptors. By contrast, olfactory and gustatory cues can, in at least some cases, be associated with a specific behavioral response simply by their detection, as the chemical identity of the pheromones, for example, can convey behaviorally relevant information. Our data demonstrate that similarly dedicated channels exist in the visual system, but since the inputs to these circuits must undergo significant upstream signal processing, many of these channels emerge late in visual circuitry.

Experimental Procedures

Electrophysiology

We recorded the spiking activity of Foma-1 neurons using targeted loose-patch recordings, while visual stimuli, generated on a high-speed monitor, were presented to the fly using two coherent fiber optic arrays. Looming stimuli comprised of either an expanding white or a black dot on a grey background. The visual angle of the dot was given by the equation $\theta(t)=2\tan^{-1}\frac{l}{vt}$, where l is half of the length of the object and v the velocity of the object towards the fly. For the single approach looming stimulus a single velocity was used for each approach, while for the random looming stimulus, the velocity was chosen from a uniform distribution every 25 ms, such that the object jittered both towards and away from the fly. A Linear-Nonlinear model was calculated through reverse correlation of the neurons' activity to the visual angle of the looming stimulus. Individual cells were filled by electroporation of Texas Red dextran, and serial optical sections were taken in the intact preparation using a confocal microscope with a water immersion objective.

Behavioral assays

To evoke loom escape behavior, individual flies were placed on a platform, presented with a single approach looming stimulus, and scored as to whether they took off in response. To block neural activity, *Shibire*^{ts}was expressed in either Foma-1 or L2 neurons, and both experimental and control genotypes were warmed to the non-permissive temperature immediately prior to experiments. Optogenetic stimulation was produced by expressing channelrhodopsin in either Foma-1, L2 or mushroom body neurons. Individual flies were placed on a platform, illuminated by 470 nm light with an irradiance of 713 W/m^2, and scored by the time of their takeoff.

See Supplemental Experimental Procedures for complete methods.

Supplementary Material

Refer to Web version on PubMed Central for supplementary material.

Acknowledgments

The authors would like to thanks Liqun Luo for fly stocks; Markus Meister, Liqun Luo, Damon Clark, Daryl Gohl and Marion Silies for comments on the manuscript; Miriam Goodman, Glenn Turner and Stephen Baccus for technical advice; and Marion Silies for dissection assistance. This work was funded by a Stanford Dean's

Fellowship (S.E.J.dV.), a NIH Director's Pioneer Award (T.R.C.DP0035350), and a McKnight Foundation Scholar's Award (T.R.C.).

References

1. Fotowat H, Gabbiani F. Collision detection as a model for sensory-motor integration. Annual Review of Neuroscience. 2011; 34:1–19.
2. Srinivasan M, Zhang S. Visual motor computations in Insects. Annual Review of Neuroscience. 2004; 27:679–696.
3. Borst A, Haag J, Reiff DF. Fly motion vision. Annual Review of Neuroscience. 2010; 33:49–70.
4. Fischbach KF, Dittrich APM. The optic lobe of *Drosophila melanogaster*. I. A Golgi analysis of wild-type structure. Cell Tissue Research. 1989; 258:441–475.
5. Otsuna H, Ito K. Systematic analysis of the visual projection neurons of *Drosophila melanogaster*. I. Lobula-specigic pathways. The Journal of Comparative Neurology. 2006; 497:928–958. [PubMed: 16802334]
6. Hausen, K. The lobula-complex of the fly: structure, function and significance in visual behaviour. In: Ali, MA., editor. Photoreception and Vision in Invertebrates. New York: Plenum; 1984. p. 523-559.
7. Nordstrom K, O'Carroll DC. Small object detection neurons in female hoverflies. Proceedings of the Royal Society B. 2006; 273:1211–1216. [PubMed: 16720393]
8. O'Carroll DC. Feature-detecting neurons in dragonflies. Nature. 1993; 362:541–543.
9. Heisenberg M, Wonneberger R, Wolf R. optomotor-blind^{H31} - a *Drosophila* mutant of the lobula plate giant neurons. Journal of Comparative Physiology. 1978; 124:287–296.
10. Blondeau J. Electrically evoked course control in the fly *Calliphora erythrocephala*. Journal of Experimental Biology. 1981; 92:143–153.
11. Geiger G, Nassel DR. Visual orientation behaviour of flies after selective laser beam ablation of interneurones. Nature. 1981; 293:398–399. [PubMed: 7278992]
12. Hausen K, Wehrhahn C. Neural circuits mediating visual flight control in flies. II. Separation of two control systems by microsurgical brain lesions. The Journal of Neuroscience. 1990; 10:351–360. [PubMed: 2299398]
13. Chichilnisky EJ. A simple white noise analysis of neuronal light responses. Network: Computation in Neural Systems. 2001; 12:199–213.
14. Marmarelis PZ, McCann GD. Development and application of white-noise modeling techniques for studies of insect visual nervous system. Kybernetik. 1973; 12:74–89. [PubMed: 4694256]
15. Card G, Dickinson MH. Visually mediated motor planning in the escape response of *Drosophila*. Current Biology. 2008; 18:1300–1307. [PubMed: 18760606]
16. Card G, Dickinson MH. Performance trade-offs in the flight initiation of *Drosophila melanogaster*. The Journal of Experimental Biology. 2008; 211:341–353. [PubMed: 18203989]
17. Fotowat H, Fayyazuddin A, Bellen HJ, Gabbiani F. A novel neuronal pathway for visually guided escape in *Drosophila melanogaster*. Journal of Neurophysiology. 2009; 102:875–885. [PubMed: 19474177]
18. Hammond S, O'Shea M. Escape flight initiation in the fly. Journal of Comparative Phsyiology A. 2007; 193:471–476.
19. Katsov AY, Clandinin TR. Motion processing streams in *Drosophila* are behaviorally specialized. Neuron. 2008; 59:322–335. [PubMed: 18667159]
20. Joesch M, Plett J, Borst A, Reiff DF. Response properties of motion-sensitive visual interneurons in the lobula plate of *Drosophila melanogaster*. Current Biology. 2008; 18:368–374. [PubMed: 18328703]
21. Hatsopoulos N, Gabbiani F, Laurent G. Elementary computation of object approach by a wide-field visual neuron. Science. 1995; 270:1000–1003. [PubMed: 15290817]
22. Gabbiani F, Mo C, Laurent G. Invariance of angular thresold computation in a wide-field looming-sensitive neuron. The Journal of Neuroscience. 2001; 21:314–329. [PubMed: 11150349]

23. Rind CF, Simmons PJ. Orthopteran DCMD neuron: a reevaluation of responses to moving objects. I. Selective responses to approaching objects. Journal of Neurophysiology. 1992; 68:1654–1666. [PubMed: 1479436]
24. Sun H, Frost BJ. Computation of different optical variable of looming objects in pigeon nucleus rotundus neurons. Nature Neuroscience. 1998; 1:296–303.
25. Wang Y, Frost BJ. Time to collision is signalled by neurons in the nucleus rotundus of pigeons. Nature. 1992; 356:236–238. [PubMed: 1552942]
26. Fotowat H, Harrison RR, Gabbiani F. Multiplexing of motor information in the discharge of a collision detecting neuron during escape behaviors. Neuron. 2011; 69:147–158. [PubMed: 21220105]
27. Liu YJ, Wang Q, Li B. Neuronal responses to looming objects in the superior colliculus of the cat. Brain, Behavior and Evolution. 2011; 77:193–205.
28. Nakagawa H, Hongjian K. Collision-sensitive neurons in the optic tectum of the Bullfrog, *Rana catesbeiana*. Journal of Neurophysiology. 2010; 104:2487–2499. [PubMed: 20810689]
29. Preuss T, Osei-Bonsu PE, Weiss SA, Wang C, Faber DS. Neural representation of object approach in a decision-making motor circuit. The Journal of Neuroscience. 2006; 26:3454–3464. [PubMed: 16571752]
30. Gabbiani F, Krapp HG, Koch C, Laurent G. Multiplicative computation in a visual neuron sensitive to looming. Nature. 2002; 420:320–324. [PubMed: 12447440]
31. Gabbiani F, Krapp HG, Laurent G. Computation of object approach by a wide-field, motion-sensitive neuron. The Journal of Neuroscience. 1999; 19:1122–1141. [PubMed: 9920674]
32. Clark DA, Bursztyn L, Horowitz MA, Schnitzer MJ, Clandinin TR. Defining the computational structure of the motion detector in *Drosophila*. Neuron. 2011; 70:1165–1177. [PubMed: 21689602]
33. Joesch M, Schnell B, Raghu SV, Reiff DF, Borst A. ON and OFF pathways in *Drosophila* motion vision. Nature. 2010; 468:300. [PubMed: 21068841]
34. Kitamoto T. Conditional modification of behavior in *Drosophila* by targeted expression of a temperature-sensitive shibire allele in defined neurons. Journal of Neurobiology. 2001; 47:81–92. [PubMed: 11291099]
35. Rister J, Pauls D, Schnell B, Ting CY, Lee CH, Sinakevitch I, Morante J, Strausfeld NJ, Ito K, Heisenberg M. Dissection of the peripheral motion channel in the visual system of *Drosophila melanogaster*. Neuron. 2007; 56:155–170. [PubMed: 17920022]
36. Suh GSB, Ben-Tabou de Leon S, Tanimoto H, Fiala A, Benzer S, Anderson DJ. Light activation of an innate olfactory avoidance response in *Drosophila*. Current Biology. 2007; 17:905–908. [PubMed: 17493811]
37. Bloomquist BT, Shortridge RD, Schneuwly S, Perdew M, Montell C, Steller H, Rubin G, Pak WL. Isolation of a putative phospholipase C gene of *Drosophila*, *norpA*, and its role in phototransduction. Cell. 1988; 54:723–733. [PubMed: 2457447]
38. Peron SP, Jones PW, Gabbiani F. Precise subcellular input retinotopy and its computational consequences in an identified visual interneuron. Neuron. 2009; 83:830–842. [PubMed: 19778511]
39. Rind CF. Non-directional, movement sensitive neurones of the locust optic lobe. Journal of Comparative Phsyiology A. 1987; 161:447–494.
40. Rowell CHF, O'Shea M, Williams JLD. The neuronal basis of a sensory analyser, the acridid movement detector system. IV. The preference for small field stimuli. Journal of Experimental Biology. 1977; 68:157–185. [PubMed: 894184]
41. Krapp HG, Gabbiani F. Spatial distribution of inputs and local receptive field properties of a wide-field, looming sensitive neuron. Journal of Neurophysiology. 2005; 93:2240–2253. [PubMed: 15548622]
42. Jones PW, Gabbiani F. Synchronized neural input shapes stimulus selectivity in a collision-detecting neuron. Current Biology. 2010; 20:1–6. [PubMed: 20036540]
43. Simmons PJ, Rind CF. Orthopteran DCMD neuron: a reevaluation of responses to moving objects. II. Critical cues for detecting approaching objects. Journal of Neurophysiology. 1992; 68:1667–1682. [PubMed: 1479437]

44. Tammero LF, Dickinson MH. The influence of visual landscape on the free flight behavior of the fruit fly *Drosophila melanogaster*. The Journal of Experimental Biology. 2002; 205:327–343. [PubMed: 11854370]

45. Tammero LF, Dickinson MH. Collision-avoidance and landing responses are mediated by separate pathways in the fruit fly, *Drosophila melanogaster*. The Journal of Experimental Biology. 2002; 205:2785–2798. [PubMed: 12177144]

46. Borst A. *Drosophila's* view on insect vision. Current Biology. 2009; 19:R36–47. [PubMed: 19138592]

Highlights

- Loom sensitive neurons in *Drosophila* respond to imminent collisions.
- Genetic silencing of loom detectors prevents normal escape behavior.
- Optogenetic stimulation of these neurons in a blind fly triggers escape.
- Defines a causal link in a sensorimotor pathway.

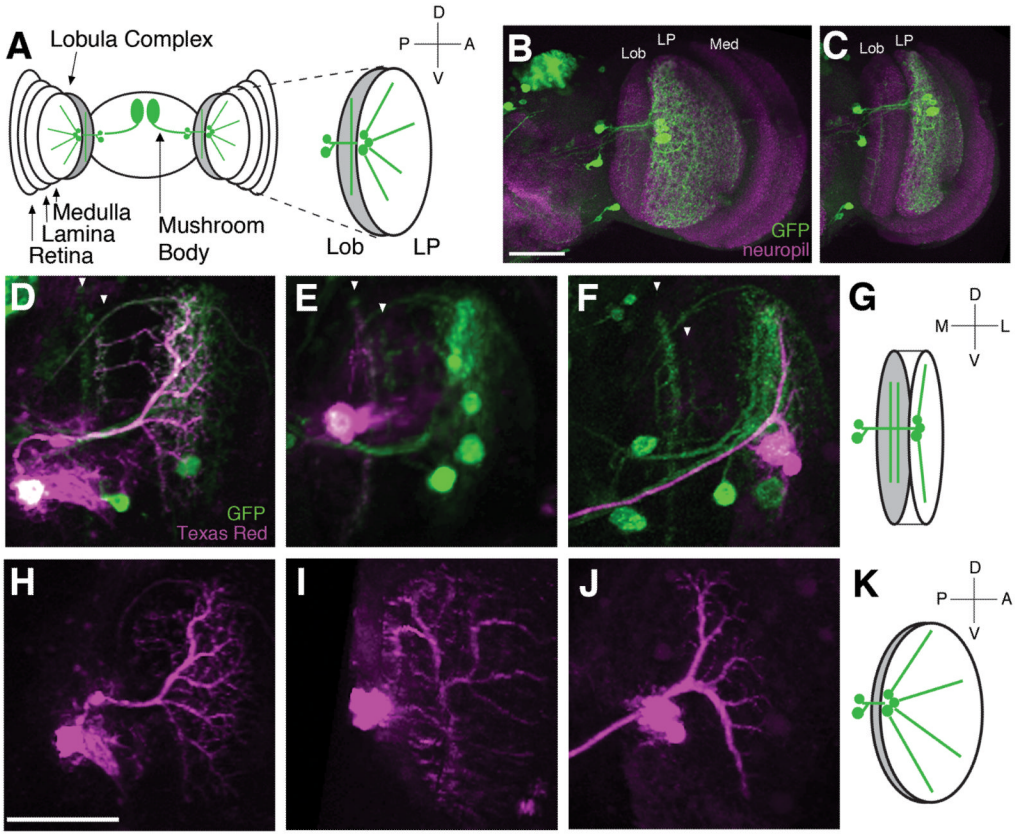

Figure 1. The Foma-1 enhancer trap labels three morphologically distinct cell types in the lobula complex

A) Schematic of the fly brain showing the expression of the Foma-1 enhancer trap in the lobula complex and mushroom bodies. The visual system comprises the retina, lamina, medulla, and the lobula complex, which consists of the lobula (Lob) and lobula plate (LP, inset). D, dorsal, V, ventral, P, posterior, A, anterior.

B) Posterior view of a confocal image of the brain labeled with a presynaptic marker (nc82, magenta) visualizing Foma-1 neurons in the lobula complex expressing GFP (green). Scale bar 50 μm.

C) A rotated view of a confocal stack of the Foma-1 neurons in the lobula complex. D–K) Confocal images of single dye labeled (magenta) Foma-1 neurons expressing GFP (green). D, H) the translobula-plate neuron, E, I) the lobula projection neuron, F, J) the lobula plate tangential cell, G, K) schematics indicating the orientation of the lobula and lobula plate in D–F and H–J respectively. M, medial, L, lateral. D–F) merged images. Arrowheads denote two layers of the lobula. H–J) single channel images of the dye. Scale bar 50 μm.

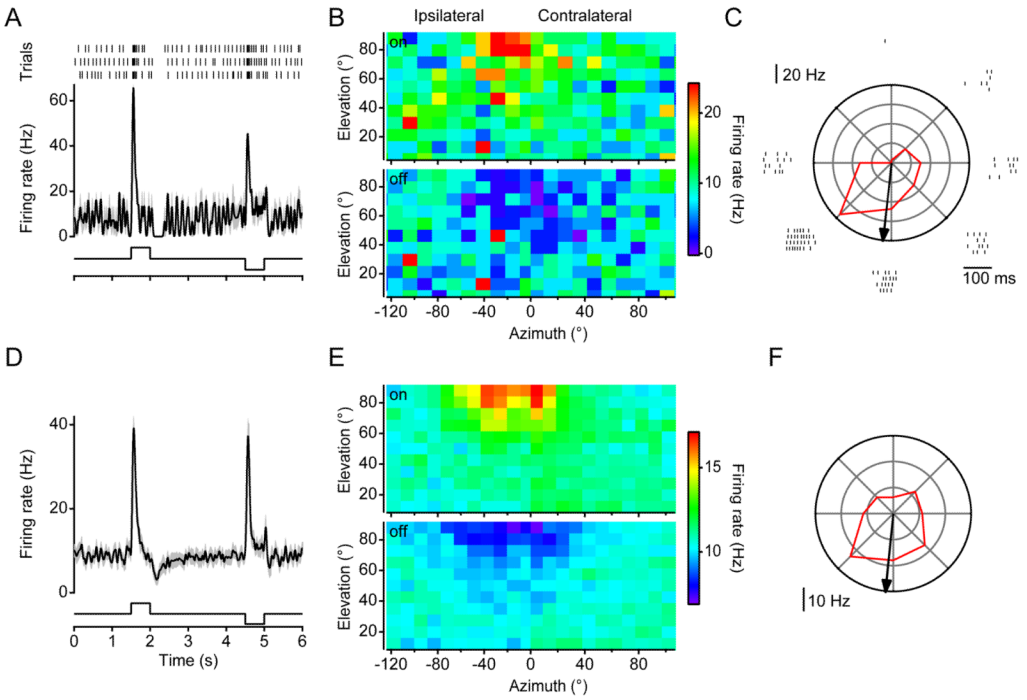

Figure 2. Foma-1 neurons are most sensitive to visual stimuli within a dorsal receptive field

A) Raster plot and averaged firing rate of a Foma-1 neuron's response to full field luminance steps. The recorded spikes were smoothed with a 20 ms Gaussian filter.

B) Receptive field of a Foma-1 neuron. A single 10° dot of light was flashed on and off three times in 242 location in the visual field. The averaged firing rate of the neuron during the light on phase (above) and light off phase (below) is plotted as a function of the dot's location.

C) Raster plots and polar plot of a Foma-1 neuron's response to the motion of a 10° dot at one position (azimuth = 24°, elevation = 55°). The average firing rate of the cell is plotted in red. The black arrow denotes the average vector for this position.

D) Averaged response to full field luminance steps (mean ± s.e.m., n = 21).

E) Averaged receptive fields during the on phase (above) and off phase (below) of Foma-1 neurons (n = 64).

F) Polar plot of averaged response to motion of a 10° dot for one position (azimuth = 24°, elevation = 55°, n = 41).

See also Figure S1.

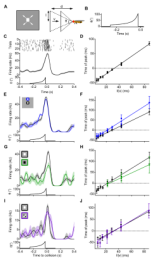

Figure 3. Foma-1 neurons detect looming stimuli

A) The looming stimulus. A dot, of size *2l*, approaches the fly at a constant velocity, *v*, from an initial distance *d*. θ denotes the visual angle of the object.

B) The visual angle of the object increases according to the equation: $\theta(t)=2\tan^{-1}\frac{l}{vt}$. Time is measured relative to the time of collision, such that $\theta\ (t=0)$ is 180°. The dot is eliminated when θ = 120°. $l/|v|$ = 22 ms.

C) Raster plot and the averaged firing rate of a Foma-1 neuron's response to the looming stimulus, averaged over 24 trials (mean ± s.e.m.). The recorded spikes were smoothed with a 20 ms Gaussian filter. Lower trace denotes stimulus. $l/|v|$ = 22 ms.

D) Time of peak response relative to the time of collision as a function of $l/|v|$ (mean ± s.e.m., n = 27).

E) Averaged responses of a Foma-1 neuron to the looming stimulus originating centrally (azimuth = 0°, elevation = 30°, black, 12 trials) or in the periphery (azimuth = 0°, elevation = 90°, blue, 12 trials) of the visual field. $l/|v|$ = 44 ms.

F) Time of peak response relative to the time of collision as a function of $l/|v|$ for looming stimuli originating in the middle (black) or the periphery (blue) of the visual field. While the firing rate peak did trend slightly earlier for the stimuli that originated in the periphery, the difference in timing was not significant for any $l/|v|$ condition (mean ± s.e.m., unpaired t test, n = 8).

G) Averaged responses of a Foma-1 neuron to looming stimuli for contrast increment (black, 11 trials) and contrast decrement (green, 3 trials). $l/|v|$ = 22 ms.

H) Time of peak response relative to the time of collision as a function of $l/|v|$ for contrast increment (black) and contrast decrement (green) looming stimuli (mean ± s.e.m., n = 4).

I) Averaged responses of a Foma-1 neuron to looming stimuli for contrast increment (black, 12 trials) and a checkerboard dot (purple, 12 trials). $l/|v|$ = 44 ms.

J) Time of peak response relative to the time of collision as a function of $l/|v|$ for a white dot (black) and a checkerboard dot (purple) looming on a grey background (mean ± s.e.m., n = 3).

See also Figure S2.

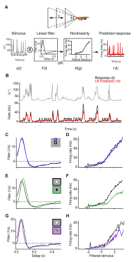

Figure 4. A Linear-Nonlinear model captures the loom response of Foma-1 neurons

A) A schematic illustration of the random looming stimulus, and of the Linear-Nonlinear (LN) model used to capture loom detector responses. The stimulus, *s(t)*, is convolved with a linear filter, *F(t)*; this output, *g(t)*, is then passed through a static nonlinearity, *N(g)*, to produce the predicted response, *r'(t)*.

B) Angular profile of the random looming stimulus (gray), the instantaneous firing rate response of a Foma-1 neuron to this stimulus (black), and the response predicted by the LN model for that neuron (red). The stimulus had a mean angle of 32°, with a standard deviation of 23°. For seven neurons analyzed with repeated stimuli, the Pearson's correlation coefficient between the predicted and actual response, 0.70 ± 0.03, was higher than that between repeated responses to the same stimulus presentations, 0.63 ± 0.04 (mean ± s.e.m.).

C) Linear filters and (D) nonlinearities for looming stimuli originating in the center (azimuth = 0°, elevation = 30°, black) and the periphery (azimuth = 0°, elevation = 90°, blue) of the visual field. Linear filter rms = 0.17 ± 0.03, nonlinearity rms = 0.15 ± 0.02 (mean ± s.e.m., n = 5, see Methods).

E) Linear filters and (F) nonlinearities for contrast increment (black) and contrast decrement (green) conditions. Linear filter rms = 0.57 ± 0.08, nonlinearity rms = 0.54 ± 0.08 (mean ± s.e.m., n = 6).

G) Linear filters and (H) nonlinearities for white dot (black) and checkerboard dot (purple) looming stimuli. Linear filter rms = 0.49 ± 0.15, nonlinearity rms = 0.48 ± 0.06 (mean ± s.e.m., n = 3).

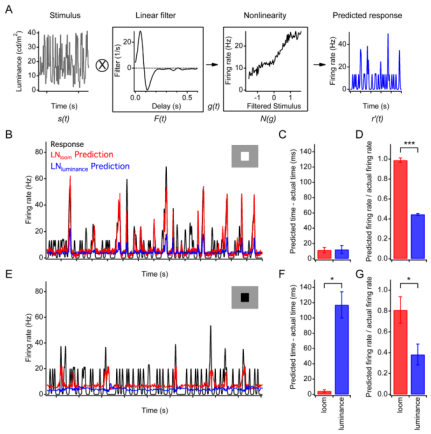

Figure 5. A LN model derived from luminance signals poorly predicts Foma-1 responses to looming

A) A schematic illustration of the full field flicker stimulus, and of the $LN_{luminance}$ model.

B) Instantaneous firing rate response to the random looming stimulus with a contrast increment (black), the responses predicted by the LN_{loom} model (Figure 4, red) and the $LN_{luminance}$ model (blue). For the $LN_{luminance}$prediction, the average luminance of the random loom stimulus was calculated for each frame, then convolved with the linear filter, and passed though the static nonlinearity, both calculated from the full field flicker stimulus. The Pearson's correlation coefficient between the LN_{loom} prediction and the actual response was 0.56 ± 0.04 (mean ± s.e.m.) while that between the $LN_{luminance}$ prediction and the actual response was 0.45 ± 0.05 (mean ± s.e.m). n = 15 cells.

C) Difference between the predicted and actual time of 20 randomly chosen peak firing events for the contrast increment random looming stimulus. LN_{loom} (red). $LN_{luminance}$ (blue). Mean ± s.e.m., n = 11 cells.

D) The ratio of the predicted peak firing rate to the actual peak firing rate for the same 20 random peak firing events as in (C). Mean ± s.e.m., n = 11, ***p<0.0001 paired t test.

E) Instantaneous firing rate response of one neuron to the random looming stimulus with a contrast decrement (black), the response predicted by the LN_{loom} model (red), and the response predicted by the $LN_{luminance}$ model (blue). Mean ± s.e.m., n = 3 cells.

F) Difference between the predicted time and the actual time of 20 randomly chosen peak firing events for the contrast decrement random looming stimulus. LN_{loom} (red). $LN_{luminance}$ (blue). Mean ± s.e.m., n = 3, *p<0.05, paired t test.

G) The ratio of the predicted peak firing rate to the actual peak firing rate for the same 20 random peak firing events as in (F). Mean ± s.e.m., n = 3, *p<0.05, paired t test.

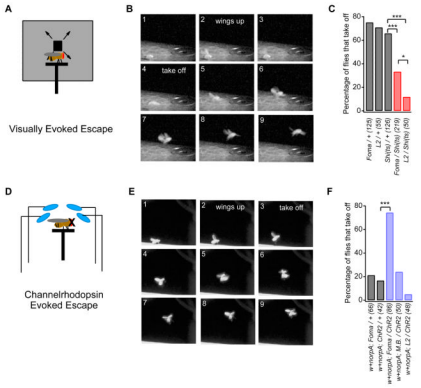

Figure 6. Foma-1 neurons are important for the escape response

A) Schematic of the experimental apparatus. Individual flies on a small platform were presented a looming stimulus of a dark square on a grey background, and scored as to whether they took off from the platform.

B) High speed video frames of a loom escape response. Frames are numbered consecutively with 5 ms between frames.

C) Percentage of flies that escaped from the looming stimulus. (*p < 0.05, ***p<0.0001, two tailed Fisher's Exact test.)

D) Schematic of experimental apparatus for optogenetic stimulation of escape behavior. Blind flies on a small platform were illuminated with intense blue light.

E) High speed video frames of an escape response evoked by channelrhodopsin stimulation. Frames are numbered consecutively with 5 ms between frames.

F) Percentage of flies that took off within 5 seconds of the onset of illumination. (***p < 10^{7-9}, two tailed Fisher's Exact test.) M.B. denotes the genetic driver expressed specifically in the mushroom body. The percentages of take offs elicited by activation of M.B. and L2 neurons were not significantly different from control (p = 0.46 and p = 0.09 respectively). See also Figure S3, Movie S1 and Movie S2.